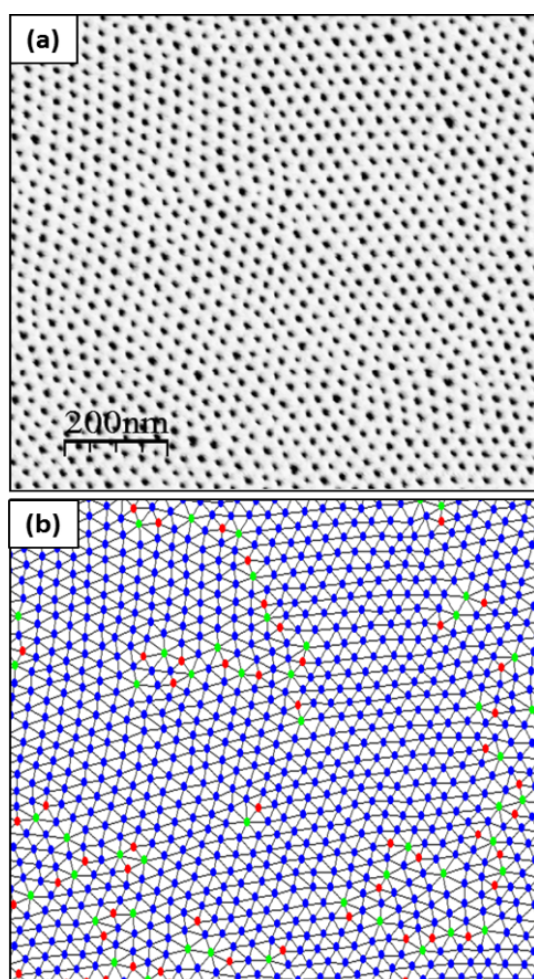


## Electronic Supplementary Information

### Hierarchical assembly of magnetic L10-ordered FePt nanoparticles in block copolymer thin films

Karim Aissou,<sup>a</sup> Thomas Alnasser,<sup>b</sup> Gilles Pecastaings,<sup>a</sup> Graziella Goglio,<sup>b</sup> Olivier Toulemonde,<sup>b</sup> Stéphane Mornet,<sup>b</sup> Guillaume Fleury,<sup>\*a</sup> and Georges Hadziioannou<sup>\*a</sup>

#### 1. Phase behavior of the neat PS-*b*-PEO thin films



**Fig S1** (a) Phase contrast SFM image of the microphase-separated neat PS-*b*-PEO thin film annealed under a toluene/water vapor saturated atmosphere which exhibits a hexagonal packing of PEO domains with an inter-cylinder spacing of 30.5 nm. The light spots, located within the spherical PEO domains of the nanocomposite thin film are not found for the neat copolymer (b) Delaunay triangulation showing well-organized grains which correspond to regions where all PEO spheres are 6-fold coordinated (blue dots). These grains are delimited by 7-fold (green dots) and 5-fold (red dots) coordinated cylinders.

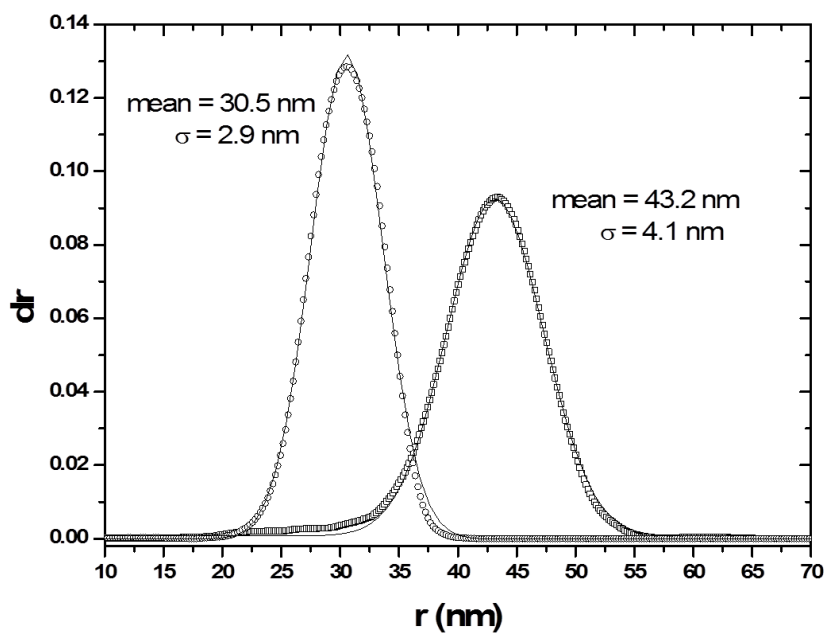


**Fig S2** Nearest-neighbor distance distribution functions for the neat PS-*b*-PEO and the PS-*b*-PEO/FePt\_mPEO-Dopa thin films. The inter-domain spacing distribution,  $d$ , obtained from the neat PS-*b*-PEO film has a sharp shape ( $d = 30.5 \pm 2.9$  nm) while the PS-*b*-PEO/FePt\_mPEO-Dopa film containing 20 wt % FePt NPs has a broad one ( $d = 43.2 \pm 4.1$  nm).

## 2. Physical properties of $L1_0$ -ordered FePt nanoparticles

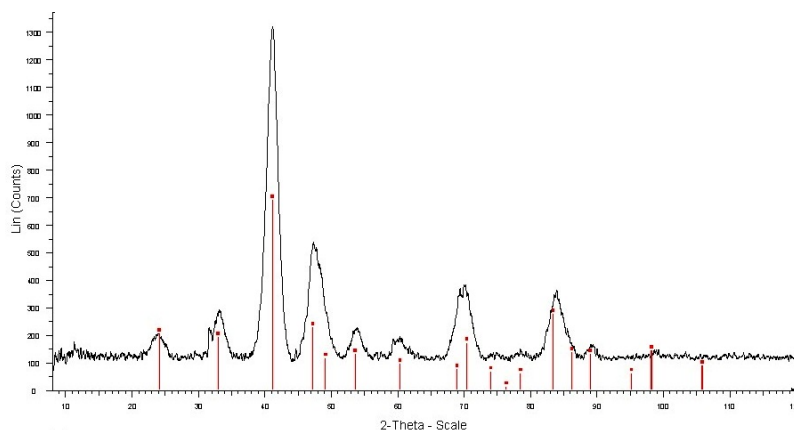


**Fig S3** XRD pattern of FePt nanoparticles. The expected peak positions for the tetragonal FePt phase are indexed and confirm the well-crystallized  $L1_0$ -ordered phase structure of the FePt NPs.

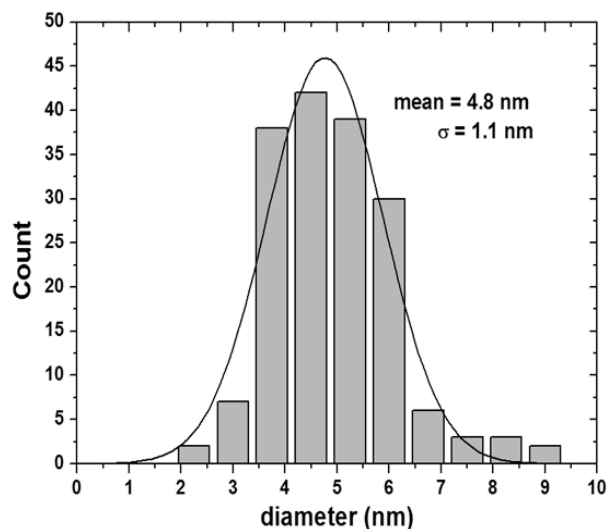


**Fig S4** Distribution of the FePt core diameter measured from the TEM image presented in Fig.1. The average core diameter is about 4.8 nm ( $\sigma = 1.1$  nm). Here,  $\sigma$  represents the standard deviation extracted from the Gaussian distribution used to fit the data.

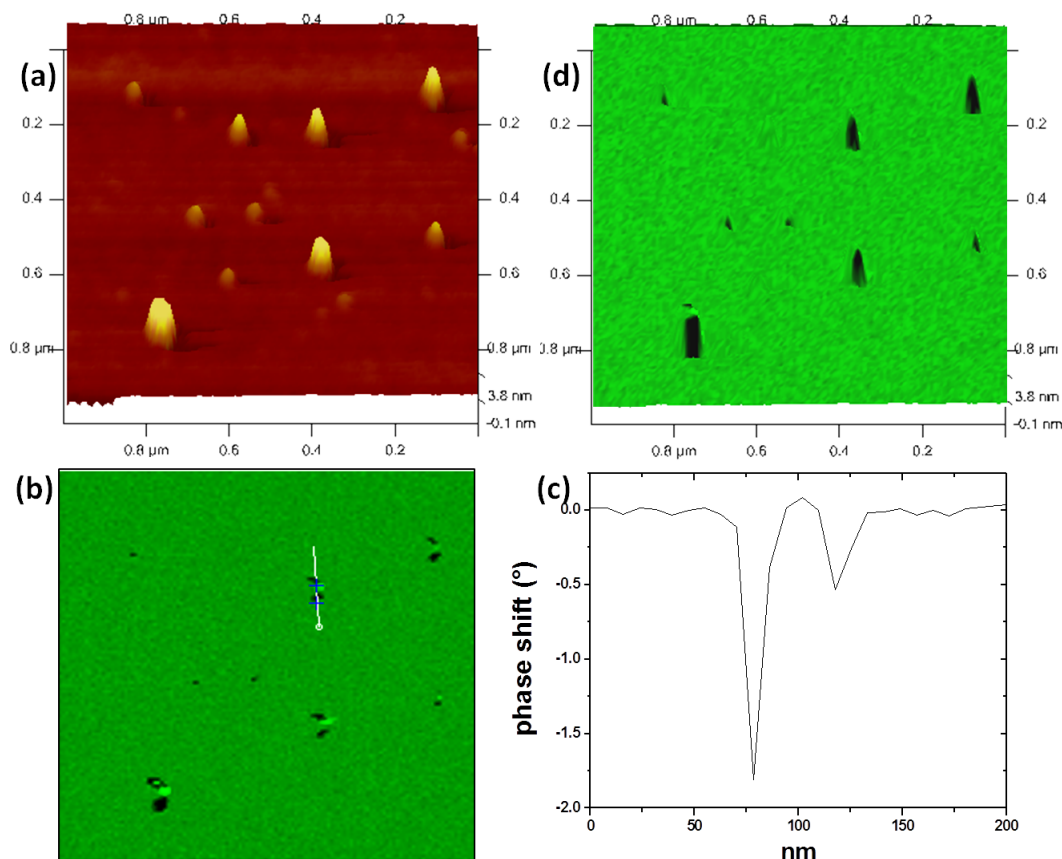


**Fig S5** (a) ( $1.0 \mu\text{m} \times 1.0 \mu\text{m}$ ) 3D-topographic SFM image (torsional mode) of small aggregates of FePt NPs deposited on a silicon substrate by drop casting from a diluted THF solution (5 wt%) and (b) its magnetic phase image obtained with a lift height of 5 nm. Each black spot corresponds to a magnetic signal which is due to the presence of a FePt NPs aggregate. (c) The magnetic phase cross-section profile corresponding to the continuous white line of the Fig. 4(b) reveals that the presence of FePt NP aggregate induces a maximum phase shift,  $\varphi_{\text{max}}$ , of  $1.8^\circ$ . (d) Composite image of topography and magnetic phase shows that each dark spot (magnetic signal) is located on a dot.

### 3. Macroscopic magnetic and MFM studies of PS-*b*-PEO/FePt\_mPEO-Dopa composite thin film

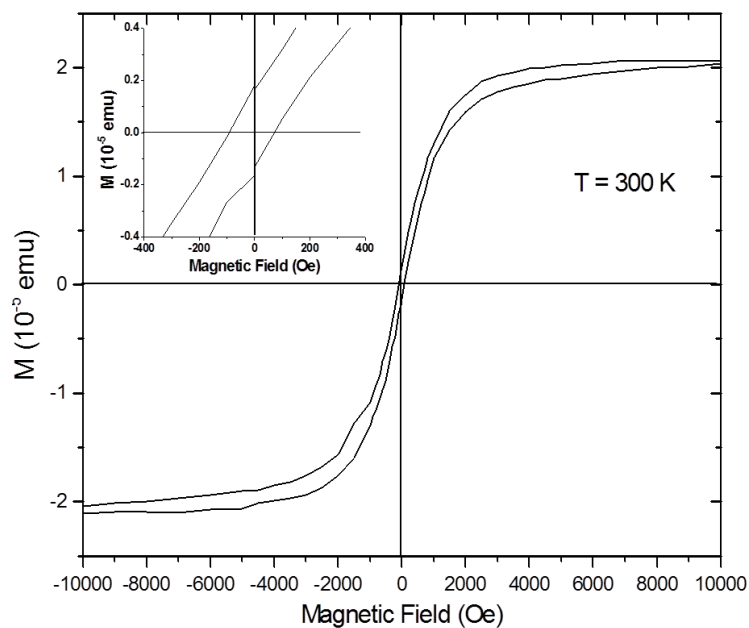


**Fig S6** Magnetic hysteresis loop of PS-*b*-PEO/FePt\_mPEO-Dopa thin film containing 20 wt % FePt NPs measured at 300K.

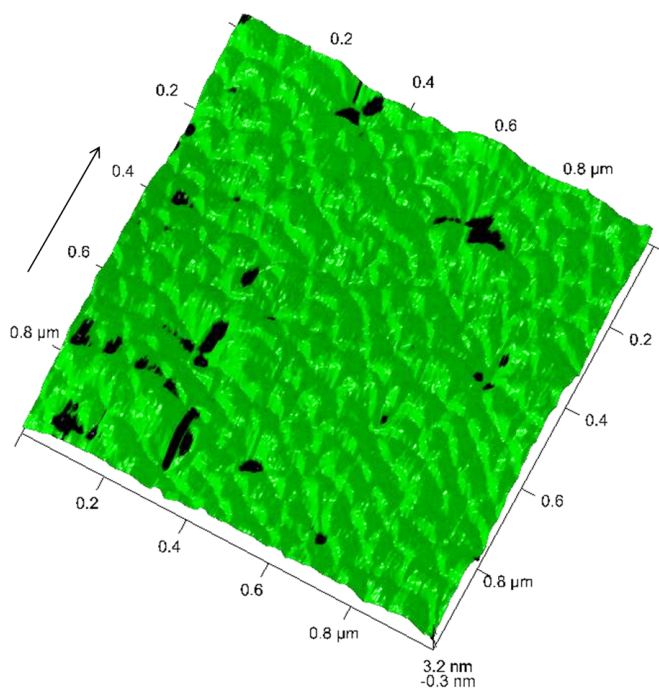


**Fig S7** ( $1.0 \mu\text{m} \times 1.0 \mu\text{m}$ ) 3D-topographic image with the magnetic phase overlay of PS-*b*-PEO/FePt\_mPEO-Dopa thin film containing 20 wt % FePt NPs obtained with a lift height of 2 nm. At this height, the magnetic phase overlay presents no indication of the topography. Most of the dark spots (magnetic signals) adopt a distorted shape along the direction of the cantilever motion (indicated by an arrow) due to the stronger interaction between the MFM tip and the FePt NPs.